

## Chain Stiffness of Elastin-Like Polypeptides

Sabine Fluegel,<sup>†</sup> Karl Fischer,<sup>†</sup> Jonathan R. McDaniel,<sup>‡</sup> Ashutosh Chilkoti,<sup>‡</sup> and Manfred Schmidt<sup>\*†</sup>

*Institute of Physical Chemistry, University of Mainz, 55099 Mainz, Germany, and Department of Biomedical Engineering, Duke University, Durham, North Carolina 27708, United States*

Received August 17, 2010

Revised Manuscript Received October 1, 2010

### Introduction

Elastin is a structural protein that is largely responsible for the elastic properties of tissues in vertebrates. It consists of alternating hydrophobic and cross-linking domains. The hydrophobic domains are dominated by hydrophobic amino acids, such as proline, valine, alanine, and leucine. The cross-linking domains contain lysyl residues combined with proline-rich regions or polyalanine domains. Elastogenesis,<sup>1</sup> the biological synthesis of elastin, involves the synthesis of a soluble precursor protein, tropoelastin, that binds to galactoselectin after its translation to prevent its intracellular aggregation. After secretion of the tropoelastin–galactoselectin complex into the extracellular space, tropoelastin is released locally and aligned at the microfibrillar scaffold.

Elastin-like polypeptides (ELP) are a class of artificial repetitive polypeptides of the pentameric repeat Val-Pro-Gly-Xaa-Gly (where Xaa is a guest residue that is any amino acid except Pro) and are so named because this motif recurs in the tropoelastin gene of most vertebrates. ELPs exhibit a lower critical solution temperature (LCST) phase transition in aqueous solution. The LCST behavior<sup>2</sup> of ELPs can be precisely specified through the control of two orthogonal variables that can be completely controlled by genetically encoded synthesis of these amino acid-based biopolymers: ELP composition, notably by the type and mole fraction of the different guest residues (X) and by the chain length. ELPs are increasingly utilized for many biomedical applications, as they are nontoxic, biodegradable, and show good pharmacokinetics.<sup>3–8</sup>

Despite extensive studies on the biophysics of ELPs,<sup>9–12</sup> there is still some controversy regarding the origins of the LCST behavior of ELPs and their elastomeric properties. Two structural models for the remarkable elasticity of elastin have been proposed; the first “ $\beta$ -spiral model”, proposed by Urry,<sup>9</sup> is based on extensive studies on synthetic poly(ValProGlyVal-Gly) and proposes that ELPs consist of a helical arrangement of type II  $\beta$ -spirals per pentameric peptide unit. The ProGly unit is positioned at the corner of the bend and a hydrogen bond connects the carbonyl group of the first valine with the amino residue of the fourth valine. The dipeptide segments of VG, suspended between the  $\beta$ -turns, exhibit large amplitude librations. The decrease of these librations upon extension results in a large decrease in entropy of the segments explaining the rubber elasticity of elastin. At variance with the classical theory of rubber elasticity, this model assumes fixed end-to-end chain lengths. Contradicting this model, molecular dynamics simulations assuming freely fluctuating ends resulted in a loss of the

**Table 1.** Calculated Molecular Weight and Hydrodynamic Radii Determined by DLS for ELP Samples

	MW/kDa	$R_h$ /nm
ELP4–120	49.4	6.0
ELP4–60	24.9	4.2
ELP4–40	16.7	3.7
ELP4–30	12.6	3.4
ELP4–20	8.5	2.7

helical  $\beta$ -spiral structure.<sup>13</sup> A second model, proposed by Tamburro et al.,<sup>14</sup> involves the formation of nonrecurring isolated type II  $\beta$ -turns for the (GlyXGlyGlyX) repeat units of the elastin sequence. The XGly or GlyGly segments build up the corners. The first and fourth glycine or the second and fifth X residue are connected via hydrogen bonds. Due to the absence of proline residues, the resulting  $\beta$ -turns can dynamically slide along the chain. The polypeptide can therefore freely fluctuate leading to high intrinsic entropy, which decreases upon extension. Both models have in common the presence of type II  $\beta$ -turns, but their dynamic interpretations are different. Molecular simulations<sup>11–13</sup> performed by Daggett and co-workers have indicated that the hydration of the hydrophobic residues largely contributes to the gain in entropy. Upon the collapse of the polypeptide the hydration water is released, thus, leading to a significant increase of solvent entropy.

The single molecule elasticity of ELP has been experimentally investigated by force microscopy as function of temperature and ionic strength.<sup>15</sup> The force distance curves were analyzed by standard expressions for a wormlike chain model, which yields the persistence length,  $l_p$ , which is connected to the Kuhn statistical segment length,  $l_k$ , by  $l_p = l_k/2$ . At  $T = 25$  °C, a very small Kuhn length was determined to  $l_k = 0.3$  nm (ELP4–120). Because it is well established that analysis of force distance curves of flexible polymers often yields values of the persistence length that are anomalously small,<sup>16</sup> a reliable determination of the chain stiffness of ELP is still missing.

### Results and Discussion

Herein, the Kuhn length of ELP was determined in dilute solution by analysis of the hydrodynamic radii ( $R_h$ ) measured by dynamic light scattering (DLS) on a series of ELPs with different molecular weights. Five ELPs Gly(Val-Pro-Gly-Val-Gly)<sub>n</sub> Phe-Cys with the guest residue valine and a single cysteine residue at the C-terminus were investigated. Their length varied from  $n = 20$  up to  $n = 120$  (notation ELP4- $n$ ), where  $n$  is the number of pentapeptide repeats. The recombinant synthesis of each ELP construct utilized plasmid reconstruction recursive directional ligation,<sup>6</sup> and is summarized along with their purification in the Supporting Information. The samples utilized are listed in Table 1.

SDS-PAGE (see Figure 1) of the ELPs was carried out to verify the purity of the ELP samples utilized in this study and DLS was utilized to determine the  $R_h$  from the measured diffusion coefficient  $D$  by application of Stokes' law

$$R_h = kT/(6\pi\eta_0 D) \quad (1)$$

where  $kT$  is the thermal energy and  $\eta_0$  is the solvent viscosity. Experimental details of the DLS measurements are in the Supporting Information (SI). Briefly, the ELPs were dissolved

\* To whom correspondence should be addressed. Fax: +49 (0)6131-3923768. E-mail: mschmidt@uni-mainz.de.

<sup>†</sup> University of Mainz.

<sup>‡</sup> Duke University.

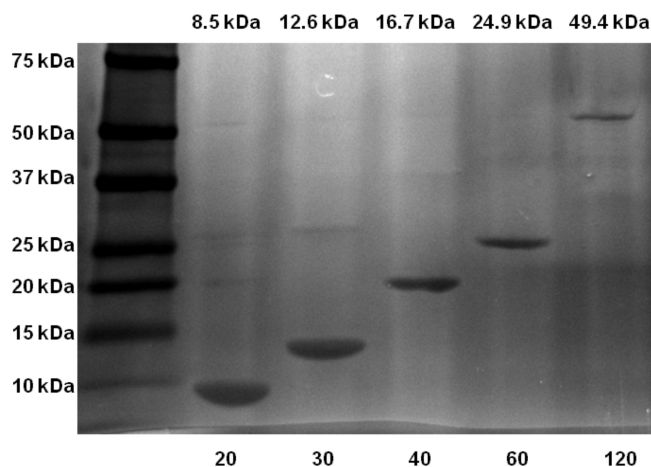


**Figure 1.** SDS-PAGE (4–20% Tris-HCl, gradient) of purified ELPs visualized by copper staining. The left lane contains a molecular weight standard, labeled in kilodaltons (kDa). The expected molecular weight is indicated on the top of each lane. The length in pentapeptides of each ELP is labeled below each lane.

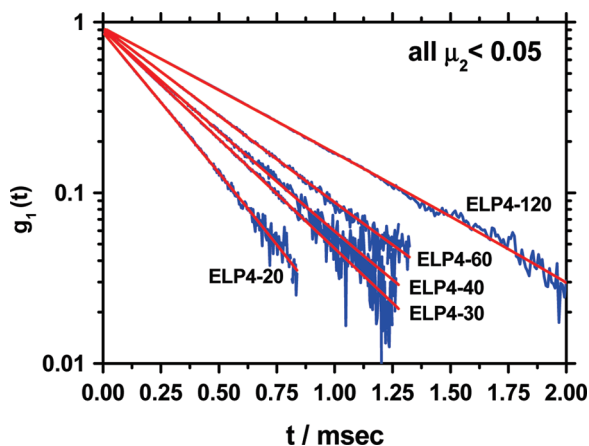


**Figure 2.** Correlation function  $g_1(t)$  of ELP4–20, ELP4–30, ELP4–40, ELP4–60, and ELP4–120 plotted vs the correlation time  $t$  in a semilogarithmic scale. The red curves represent a single exponential fit to the data in a time regime where  $g_1(t) > 0.2$ .

in 20 mM NaCl, pH = 6.5, for the LS measurements at a concentration of 5 mg/mL. This small concentration effectively represents the infinite dilution limit, because  $R_h$  of sample ELP4–40 did not change when diluted to  $c = 0.5$  g/L. All measurements were performed at a scattering angle of  $30^\circ$ . Due to the terminal cysteine group of the ELPs used in the present work, dimerization by formation of disulfide bridges is possible. Therefore, all samples were measured directly after dissolution. Control measurements revealed that dimerization noticeably starts after only 24 h.

The correlation functions for all ELP samples decayed single exponentially for  $g_1(t) > 0.2$  (Figure 2). If a cumulant fit is applied, the normalized second cumulant  $\mu_2$ , a measure for the polydispersity of the sample, is negligible, that is,  $\mu_2 < 0.05$ , which is within experimental error the expected range for monodisperse samples. In Figure 3, the double logarithmic plot of the hydrodynamic radius,  $R_h$ , of the ELPs versus the number of repeat units,  $P$ , is shown. A quantitative analysis of the data was performed by application of the Kratky–Porod wormlike chain model for the calculation of the hydrodynamic radius, as described in detail elsewhere.<sup>17</sup> Briefly, the segment distribution function derived by Koyama<sup>18</sup> was applied to numerically calculate  $R_h$ . The results are in perfect agreement with the Yamakawa–Fujii theory<sup>19,20</sup> for wormlike cylinders.

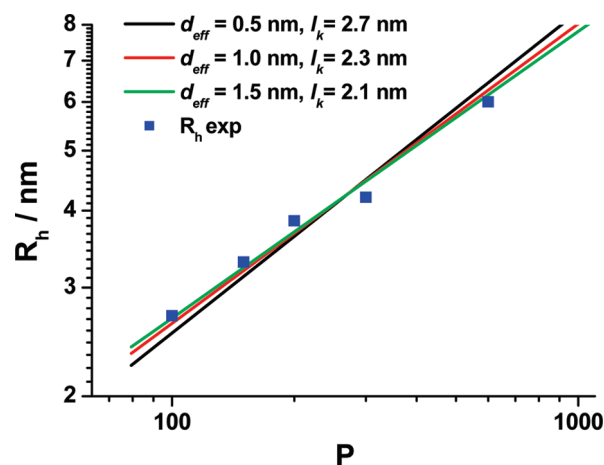


**Figure 3.** Double logarithmic plot of the hydrodynamic radius  $R_h$  vs the number of peptide repeat units  $P$ . The lines represent the best fits to the data assuming a repeat unit length  $b = 0.365$  nm: black line,  $d_{\text{eff}} = 0.5$  nm,  $l_k = 2.7$  nm; red line,  $d_{\text{eff}} = 1.0$  nm,  $l_k = 2.3$  nm; green line,  $d_{\text{eff}} = 1.5$  nm,  $l_k = 2.1$  nm.

The Kuhn statistical length  $l_k$  is obtained by fitting the calculated  $R_h$  to the measured  $R_h$  values. The parameters needed for the fit are the length per repeat unit  $b$  and the effective chain cross-section  $d_{\text{eff}}$ . The calculated fits were obtained by assuming  $b = 0.365$  nm, which was estimated from the well-known peptide bond lengths and angles<sup>21</sup> and by assuming different values for the effective chain cross-section  $d_{\text{eff}}$  of 0.5, 1.0, and 1.5 nm, which are impossible to exactly calculate for non rigid particles. Given the different side chain sizes of the amino acids in ELPs, the chosen  $d$  values include the extremes of a very small hydrodynamic effect of the side chain ( $d_{\text{eff}} = 0.5$  nm) and a maximum effect reflecting the maximum extension of the largest amino acid side chain (valine). The data are fitted best by  $d_{\text{eff}} = 1.5$  nm and  $l_k = 2.1$  nm, although the experimental data would also be compatible with  $d_{\text{eff}} = 1$  nm and  $l_k = 2.3$  nm (see separate plots and linear presentation of the data in the Supporting Information). This somewhat large value of  $d_{\text{eff}}$  could be either due to an additional hydration shell or could be caused by thicker chain regions originating from intramolecular superstructures like hair pins. The latter is unlikely as revealed by a recent simulation study combined with NMR investigations, which have highlighted the role of proline for the conformational change of ELP with temperature.<sup>22</sup> At  $T = 283$  K, no evidence for intramolecular interactions are found, whereas at  $T = 303$  K,  $\beta_{\text{II}}$ -type turns may emerge. The data in the present work were recorded at  $T = 293$  K, where ELP most probably exhibits an “unstructured” conformation.

It should be noted that  $l_k = 2.1$  nm is much larger than the previously reported  $l_k \leq 0.4$  nm derived from force–distance curve analysis in AFM measurements of single ELP molecules.<sup>15</sup> This discrepancy is not entirely unexpected, as AFM has been reported to yield extremely small Kuhn lengths that are physically anomalous.<sup>16</sup>

## Conclusion

The present work has investigated the chain stiffness of ELP at temperatures well below the LCST based on the interpretation of the hydrodynamic radii by the Yamakawa–Fujii theory of wormlike chains. The value for the Kuhn statistical segment length,  $l_k = 2.1$  nm, compares well with those reported for other water-soluble flexible polymers such as PEO<sup>23</sup> ( $l_k = 2$  nm), single-stranded RNA<sup>24</sup> ( $l_k = 2$  nm), or other coiled polypeptides like poly(sodium-L-glutamat)<sup>25</sup> ( $l_k = 1.2$  nm) or denatured

bovine A1 basic protein<sup>26</sup> ( $l_k = 3.1$  nm). As discussed above, the contour length utilized in the present analysis ignores possible secondary structures of ELP such as helices, hair pins, and so on. Because such effects would shorten the contour length leading to an increase in the Kuhn length and, accordingly, the value reported herein constitutes a minimum value of the Kuhn length of ELPs.

Unfortunately, the present results do not provide a better understanding of the LCST behavior of ELP as function of temperature or pH nor is the presented wormlike chain analysis applicable to folded or even compact rigid ELP conformations, which are expected to form close to the LCST transition. Although hydrodynamic theories are well developed, for instance, for rigid and flexible rods,<sup>27,28</sup> it would be difficult to consistently derive meaningful values for the contour length and the thickness, given the huge number of possible rigid conformations.

**Acknowledgment.** This work was supported by the DFG Priority Programm SPP 1259 (M.S.), the Graduate School of Excellence MAINZ (M.S.), and by the National Institutes of Health through Grant No. GM61232 (A.C.).

**Supporting Information Available.** Synthesis of ELP, expression and purification of ELP, SDS-Page analysis, light scattering characterization, and various plots of the data shown in Figure 3. This material is available free of charge via the Internet at <http://pubs.acs.org>.

## References and Notes

- (1) Debelle, L.; Tamburro, A. M. *Int. J. Biochem. Cell Biol.* **1999**, *31*, 261–272.
- (2) Meyer, D. E.; Chilkoti, A. *Biomacromolecules* **2004**, *5*, 846–851.
- (3) MacKay, J. A.; Chen, M. N.; McDaniel, J. R.; Liu, W. G.; Simnick, A. J.; Chilkoti, A. *Nat. Mater.* **2009**, *8*, 993–999.
- (4) Chow, D.; Nunalee, M. L.; Lim, D. W.; Simnick, A. J.; Chilkoti, A. *Mater. Sci. Eng., R* **2008**, *62*, 125–155.
- (5) Mackay, J. A.; Chilkoti, A. *Int. J. Hyperthermia* **2008**, *24*, 483–495.
- (6) McDaniel, J. R.; MacKay, J. A.; Quiroz, F. G.; Chilkoti, A. *Biomacromolecules* **2010**, *11*, 944–952.
- (7) Meyer, D. E.; Chilkoti, A. *Biomacromolecules* **2002**, *3*, 357–367.
- (8) Dandu, R.; Von Cresce, A.; Briber, R.; Dowell, P.; Cappello, J.; Ghandehari, H. *Polymer* **2009**, *50*, 366–374.
- (9) Urry, D. W.; Parker, T. M. *J. Muscle Res. Cell Motil.* **2002**, *23*, 543–559.
- (10) Tamburro, A. M. *Nanomedicine* **2009**, *4*, 469–487.
- (11) Li, B.; Alonso, D. O. V.; Daggett, V. *J. Mol. Biol.* **2001**, *305*, 581–592.
- (12) Li, B.; Daggett, V. *J. Muscle Res. Cell Motil.* **2002**, *23*, 561–573.
- (13) Li, B.; Alonso, D. O. V.; Bennion, B. J.; Daggett, V. *J. Am. Chem. Soc.* **2001**, *123*, 11991–11998.
- (14) Tamburro, A. M.; Guantieri, V.; Pandolfo, L.; Scopa, A. *Biopolymers* **1990**, *29*, 855–870.
- (15) Valiaev, A.; Lim, D. W.; Schmidler, S.; Clark, R. L.; Chilkoti, A.; Zauscher, S. *J. Am. Chem. Soc.* **2008**, *130*, 10939–10946.
- (16) Janshoff, A.; Neitzert, M.; Oberdorfer, Y.; Fuchs, H. *Angew. Chem., Int. Ed.* **2000**, *39*, 3213–3237.
- (17) Schmidt, M. *Macromolecules* **1984**, *17*, 553–560.
- (18) Koyama, R. *J. Phys. Soc. Jpn.* **1973**, *34*, 1029–1038.
- (19) Yamakawa, H.; Fujii, M. *Macromolecules* **1973**, *6*, 407–415.
- (20) Yamakawa, H.; Fujii, M. *Macromolecules* **1974**, *7*, 649–654.
- (21) Voet, D.; Voet, J. G. *Biochemie*; 1. korr. Nachdr. der 1. Aufl. ed.; VCH: Weinheim, 1994.
- (22) Glaves, R.; Baer, M.; Schreiner, E.; Stoll, R.; Marx, D. *ChemPhysChem* **2008**, *9*, 2759–2765.
- (23) Kawaguchi, S.; Imai, G.; Suzuki, J.; Miyahara, A.; Kitano, T. *Polymer* **1997**, *38*, 2885–2891.
- (24) Caliskan, G.; Hyeon, C.; Perez-Salas, U.; Briber, R. M.; Woodson, S. A.; Thirumalai, D. *Phys. Rev. Lett.* **2005**, *95*.
- (25) Shimizu, S.; Muroga, Y.; Hyono, T.; Kurita, K. *J. Appl. Crystallogr.* **2007**, *40*, S553–S557.
- (26) Krigbaum, W. R.; Hsu, T. S. *Biochemistry* **1975**, *14*, 2542–2546.
- (27) Adamczyk, Z.; Sadlej, K.; Wajnryb, E.; Ekiel-Jezewska, M. L.; Warszynski, P. *J. Colloid Interface Sci.* **2010**, *347*, 192–201.
- (28) Mansfield, M. L.; Douglas, J. F. *Macromolecules* **2008**, *41*, 5412–5421.

BM100965Y